JOM 23755

Synthesis, structure and solution conformation of some $[(\eta^5\text{-indenyl})(I_{2-n})(R)(L_n)Co^{III}]^{(n-1)+}$ ($n = 1, 2$; R = perfluoroalkyl; L = P-donor) complexes

Zhongxin Zhou, Chet Jablonski and John Bridson

Department of Chemistry, Memorial University of Newfoundland, St. John's, Newfoundland, A1B 3X7 (Canada)

(Received January 11, 1993; in revised form March 26, 1993)

Abstract

Reaction of (η^5-indenyl)(I)(R)(CO)Co (R = C_3F_7, C_6F_{13}) with P-donor ligands yields a series of mono- and disubstituted products $[(\eta^5\text{-indenyl})(I_{2-n})(R)(L_n)Co]^{(n-1)+}$ ($n = 1$, 2, L = PMe_3; $n = 1$, L = $PPhMe_2$, PPh_2Me, $PPh_2(OMe)$, PPh_3). Product distribution is highly ligand dependent and no disubstituted product forms for bulky P-donor ligands. Solution NMR data (^1H, ^{13}C, ^{19}F) for the racemic, Co-chiral, monosubstituted derivatives support a slightly distorted η^5-indenyl piano stool structure with a preferred conformation which places the perfluoroalkyl group *trans* to the indenyl 6-ring. The structure of $[(C_9H_7)(C_3F_7)(PMe_3)_2Co]I \cdot 0.5\ CH_2Cl_2$ (**5**) was determined by single crystal X-ray diffraction. Compound **5** crystallizes in the monoclinic space group $P2_1/n$ with $a = 16.760(5)$ Å, $b = 10.614(7)$ Å, $c = 28.595(5)$ Å, $\beta = 96.61(2)°$, $V = 5053(3)$ Å^3, $Z = 4$ and was refined to $R = 0.040$ and $R_w = 0.036$ based on 4097 observations with $I > 3.00\sigma(I)$.

1. Introduction

π-Indenyl complexes have attracted a great deal of attention in recent years [1–15] since they characteristically display enhanced reactivity in ligand substitution and related reactions [16–29] and catalysis [5,30–33] compared to their isostructural cyclopentadienyl derivatives. The enhanced reactivity or "indenyl effect" has been interpreted on the basis of the ability of the π-indenyl ligand to undergo facile $\eta^5 \leftrightarrow \eta^3$ "ring-slippage" [20,23–25,27,34–42]. In the course of our search for organometallic chiral auxiliaries with efficient chiral induction to coordinated phosphorus, we prepared a series of (η^5-indenyl)(I)(R)(L)Co (R = perfluoroalkyl; L = CO, P-donor) complexes [43,44] which demonstrated a strong conformational preference. The dominant solution and solid state conformation in these derivatives places perfluoroalkyl *trans* to the indenyl 6-ring and L between H_1 and H_7, *trans* to the H_3 proton of indenyl-ring as shown in Scheme 1. Good linear correlations between indenyl proton chemical shifts and electronic parameters of phosphorus ligands were demonstrated [44]. Here we report the synthesis, spectroscopic properties and solution conformation of an extended series of phosphine substituted analogs designed to test the generality of these observations.

Correspondence to: Professor C. Jablonski.

2. Results and discussion

2.1. Synthesis and characterization of the $[(\eta^5\text{-indenyl})(I_{2-n})(R)(L_n)Co]^{(n-1)+}$ ($n = 1$, 2) complexes

The title complexes were synthesized by simple substitution as shown in Scheme 2. The known complexes **1** and **2** were readily prepared [43,44] *via* oxidative addition of RI (R = C_3F_7, C_6F_{13}) to (η^5-indenyl)$(CO)_2Co$ [43,45]. Facile, ambient temperature CO substitution in **1** and **2** in non-polar solvents by a stoichiometric amount of phosphine ligand provided rac-$[(\eta^5\text{-indenyl})(I_{2-n})(R)(L_n)Co]^{(n-1)+}$ ($n = 1$, **3**, **4**, and **6–11**) in excellent (> 80%) yield. Lower conversions were realized in the case of bulky PPh_3, **12**. In contrast, the small, strongly nucleophilic phosphorus donor ligand PMe_3 lead to stepwise disubstitution of CO and I^- in **1**. Treatment of **1** with 2 equiv. of PMe_3 gave $[(\eta^5\text{-indenyl})(I_{2-n})(R)(L_n)Co]^{(n-1)+}$ ($n = 2$, **5**) as a red crystalline salt in > 90% isolated yield.

0022-328X/93/$6.00

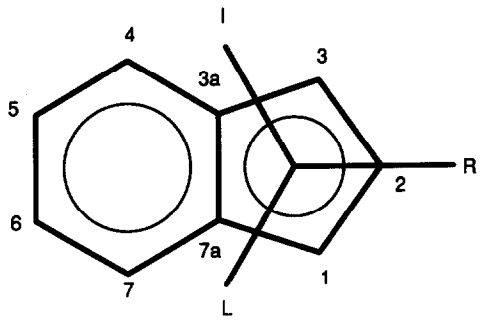

Scheme 1.

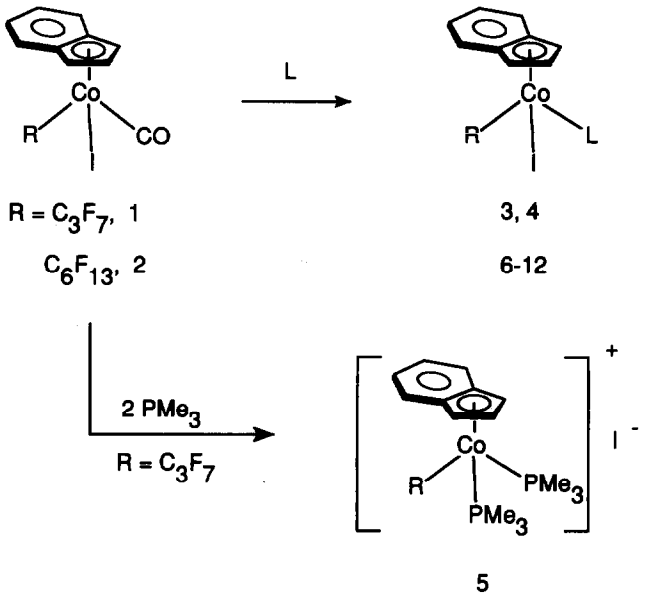

Scheme 2.

All the indenyl Co^{III} complexes prepared in this study are air stable in the solid state but decompose gradually over a period of days in solution at room temperature. The new complexes prepared have been characterized by elemental analysis, multinuclear NMR spectroscopy, and, in the case of **5**, X-ray crystallography. Their physical properties are summarized in Table 1. NMR spectra are discussed in more detail below.

2.2. Crystal structure of [(η^5-indenyl)(C_3F_7)(PMe_3)$_2$Co]I · 0.5 CH_2Cl_2 (5)

^1H and ^{13}C NMR characterization of the product obtained by reaction of **1** with 2 equiv. of PMe_3 (*cf.* Tables 4,5) revealed the presence of a symmetry plane bisecting the indenyl rings consistent with formulation as [(η^5-indenyl)(C_3F_7)(PMe_3)$_2$Co]I. A single crystal X-ray study using a deep-red prism grown by slow diffusion of hexane onto a methylene chloride solution confirmed the structure as [(η^5-indenyl)(C_3F_7)-(PMe_3)$_2$Co]I · 0.5 CH_2Cl_2 (**5**) (*cf.* Fig. 1). Details of the structure solution are provided in the Experimental section. The solid state structure shows two chemically identical but crystallographically distinct molecules, **5**, **5′**, which share a CH_2Cl_2 solvent molecule. Although we can anticipate unequal population of both rotamers in solution, rapid rotation of Co(PMe_3)$_2$(C_3F_7) establishes the time average symmetry plane required by NMR data.

The solid state conformations of the pseudooctahedral molecules **5** and **5′** are remarkably distinct, however they share a common, distorted octahedral, coordination sphere with η^5-indenyl occupying three *facial* coordination sites. Accordingly, the interligand bond angles (P(1)–Co(1)–P(2), P(1)–Co(1)–C(8), F(2)–Co(1)–C(8) for **5** and P(1′)–Co(1′)–P(2′), P(1′)–Co(1′)–C(8′), P(2′)–Co(1′)–C(8′) for **5′**) are all close to 90°. Atomic coordinates and selected bond lengths/angles for **5** and **5′** are given in Tables 2 and 3, respectively. Compound **5** (Fig.1(a)) adopts a conformation which places the C_3F_7 group *trans* to the indenyl 6-ring, but **5′** (Fig. 1(b)) prefers a conformation

TABLE 1. Physical properties of η^5-indenyl Co^{III} complexes

Compound	Complex	Yield [a] (%)	Appearance	m.p. [b] (°C)	Anal. (C, H%) Calc. (Found)
3	(C_9H_7)(C_3F_7)(I)(PMe_3)Co	81	Black rect. plate	128–129	32.99(32.59), 2.95(2.89)
4	(C_9H_7)(C_6F_{13})(I)(PMe_3)Co	86	Black rect. plate	153–154	31.06(31.18), 2.32(2.15)
5	[(C_9H_7)(C_3F_7)(PMe_3)$_2$Co]I	94	Deep-red prism	138–140	33.43(33.17), 3.94(3.98)c
6	(C_9H_7)(C_3F_7)(I)($PPhMe_2$)Co	92	Black rect. plate	120–122	39.50(39.48), 2.98(2.99)
7	(C_9H_7)(C_6F_{13})(I)($PPhMe_2$)Co	88	Black rect. plate	135–136	36.44(36.40), 2.39(2.31)
8	(C_9H_7)(C_3F_7)(I)(PPh_2Me)Co	94	Black rect. plate	111–112	44.80(45.21), 3.01(3.09)
9	(C_9H_7)(C_6F_{13})(I)(PPh_2Me)Co	95	Black rect. plate	105–106	41.00(41.44), 2.46(2.20)
10	(C_9H_7)(C_3F_7)(I)(PPh_2(OMe))Co	92	Deep-red powder	106–107	43.76(44.06), 2.94(3.15)
11	(C_9H_7)(C_8F_{13})(I)(PPh_2(OMe))Co	87	Deep-red powder	82– 84	40.22(40.26), 2.41(2.58)
12	(C_9H_7)(C_3F_7)(I)(PPh_3)Co	23	Brown powder	115–117	49.20(49.19), 3.03(2.94)

[a] Yield before crystallization. [b] Sealed N_2 capillary. [c] Analyzed as [(C_9H_7)Co(C_3F_7)(PMe_3)$_2$]I · 0.5 CH_2Cl_2.

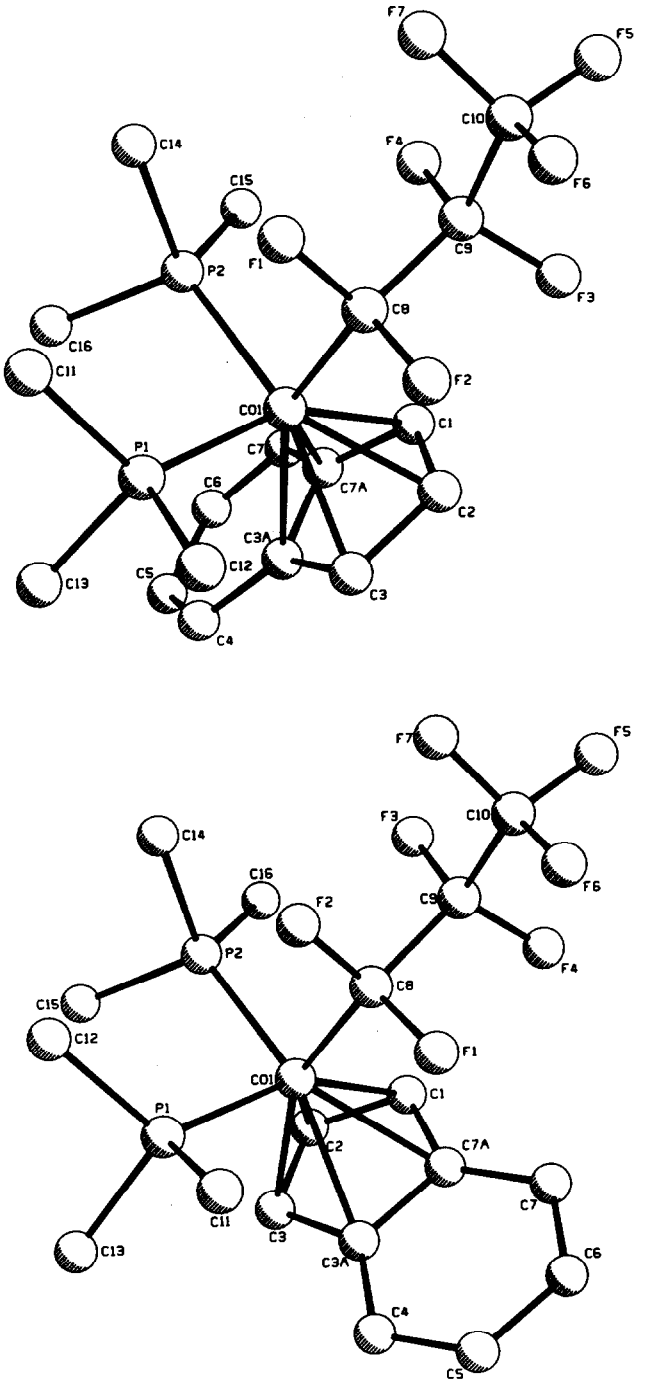

Fig. 1. (a) PLUTO diagram of [(η^5-C_9H_7)(C_3F_7)(PMe_3)$_2$Co]$^+$ (**5**). (b) PLUTO diagram of [(η^5-C_9H_7)(C_3F_7)(PMe_3)$_2$Co]$^+$ (**5′**).

in which one PMe_3 group is *trans* to the indenyl 6-ring while the C_3F_7 group is *trans* to C(3).

Consistent with their 18e$^-$ configurations, the indenyl ring is η^5 bonded in both **5** and **5′** but shows a characteristic displacement of the metal away from the C_{3a}–C_{7a} ring junction and distortions of the 5-membered ring from planarity as observed in other formally η^5-indenyl complexes [6,37,38,46,47]. Co displacement

TABLE 2. Atomic coordinates for [(η^5-C_9H_7)(C_3F_7)(PMe_3)$_2$Co]I·0.5CH_2Cl_2 (**5** and **5′**)

Atom	x	y	z	B_{eq}
I(1)	0.38906(4)	0.15836(6)	0.74481(2)	3.71(3)
I(2)	0.10274(4)	0.24785(7)	0.47472(3)	5.88(4)
Co(1)	0.68633(7)	0.2084(1)	0.40045(4)	2.73(5)
Co(1′)	0.40499(6)	0.2533(1)	0.19398(4)	2.56(5)
Cl(1)	0.8305(2)	0.0961(4)	0.8765(1)	9.9(2)
Cl(2)	0.8587(2)	0.3609(4)	0.8935(1)	9.4(2)
P(1)	0.8193(1)	0.2335(2)	0.42483(8)	3.3(1)
P(1′)	0.4242(1)	0.0986(2)	0.14141(8)	3.2(1)
P(2)	0.6772(2)	0.0082(2)	0.42089(9)	3.6(1)
P(2′)	0.3951(1)	0.4143(2)	0.14271(8)	3.2(1)
F(1)	0.6701(3)	0.4094(5)	0.4602(2)	4.3(3)
F(1′)	0.2541(3)	0.2040(5)	0.1427(2)	4.0(2)
F(2)	0.7076(3)	0.2395(5)	0.4999(2)	4.4(3)
F(2′)	0.2749(3)	0.1007(5)	0.2092(2)	4.6(3)
F(3)	0.5488(3)	0.1454(6)	0.4739(2)	6.3(3)
F(3′)	0.2431(3)	0.2993(6)	0.2589(2)	6.0(3)
F(4)	0.5195(3)	0.3288(6)	0.4444(2)	5.4(3)
F(4′)	0.2469(3)	0.4286(5)	0.2000(2)	5.7(3)
F(5)	0.4800(4)	0.3127(7)	0.5291(2)	8.0(4)
F(5′)	0.1005(4)	0.3636(8)	0.2234(2)	9.3(5)
F(6)	0.5827(5)	0.4314(8)	0.5310(3)	10.8(6)
F(6)′	0.1180(4)	0.1737(8)	0.2048(3)	9.9(5)
F(7)	0.5935(5)	0.241(1)	0.5569(2)	11.7(6)
F(7′)	0.1189(4)	0.3190(8)	0.1545(2)	8.9(4)
C(1)	0.5801(5)	0.2251(9)	0.3547(3)	3.7(5)
C(1′)	0.4230(5)	0.3442(9)	0.2592(3)	3.4(4)
C(2)	0.6353(6)	0.1465(8)	0.3346(3)	3.5(4)
C(2′)	0.4108(5)	0.214(1)	0.2650(3)	3.5(5)
C(3)	0.7043(5)	0.2151(8)	0.3291(3)	3.3(4)
C(3A)	0.6901(5)	0.3445(9)	0.3411(3)	3.0(4)
C(3′)	0.4728(5)	0.1488(8)	0.2466(3)	3.2(4)
C(3A′)	0.5292(5)	0.2401(9)	0.2338(3)	3.1(4)
C(4)	0.7346(6)	0.457(1)	0.3366(3)	4.4(5)
C(4′)	0.6074(6)	0.232(1)	0.2202(3)	4.1(5)
C(5)	0.7009(7)	0.568(1)	0.3454(4)	5.4(6)
C(5′)	0.6520(6)	0.338(1)	0.2171(3)	5.5(6)
C(6)	0.6223(8)	0.575(1)	0.3593(4)	5.2(6)
C(6′)	0.6204(8)	0.457(1)	0.2267(4)	5.3(6)
C(7)	0.5777(6)	0.471(1)	0.3657(3)	4.3(5)
C(7A)	0.6114(5)	0.3511(8)	0.3561(3)	2.9(4)
C(7′)	0.5461(7)	0.472(1)	0.2388(3)	4.4(5)
C(7A′)	0.4983(5)	0.3636(9)	0.2424(3)	3.3(5)
C(8)	0.6583(5)	0.2792(8)	0.4598(3)	3.3(5)
C(8′)	0.2891(5)	0.2170(8)	0.1896(3)	3.3(4)
C(9)	0.5721(6)	0.267(1)	0.4750(3)	4.1(5)
C(9′)	0.2314(6)	0.309(1)	0.2114(3)	4.1(5)
C(10)	0.5587(8)	0.315(1)	0.5239(4)	6.4(8)
C(10′)	0.1409(7)	0.290(1)	0.1985(5)	5.9(7)
C(11)	0.8459(6)	0.389(1)	0.4482(3)	4.7(5)
C(11′)	0.3745(6)	0.1057(9)	0.0813(3)	4.5(5)
C(12)	0.8684(5)	0.134(1)	0.4712(3)	4.6(5)
C(12′)	0.3959(6)	−0.0574(8)	0.1594(3)	5.0(5)
C(13)	0.8861(5)	0.214(1)	0.3794(3)	4.5(5)
C(13′)	0.5270(6)	0.072(1)	0.1307(4)	5.6(6)
C(14)	0.6959(6)	−0.0387(8)	0.4820(3)	4.2(5)
C(14′)	0.3126(5)	0.4214(9)	0.0957(3)	4.0(5)
C(15)	0.7454(6)	−0.0909(9)	0.3921(3)	5.0(5)
C(15′)	0.3919(6)	0.5740(8)	0.1663(3)	4.9(5)
C(16)	0.5813(6)	−0.0670(9)	0.4027(4)	5.4(6)
C(16′)	0.4832(6)	0.4216(9)	0.1100(3)	4.5(5)
C(17)	0.8205(7)	0.220(1)	0.9146(4)	8.9(9)

towards C_1–C_3 (Δ(M–C) = average of d(M–C_{3a},C_{7a}) - average of d(M–C_1,C_3)) is 0.15 Å for **5** and 0.18 Å for **5'**. Hinge angles, defined by the intersection of the planes C_1–C_2–C_3 and C_1–C_3–C_{3a}–C_{7a}, of 6.8° for **5** and 6.6° for **5'** as well as fold angles between the plane C_1–C_2–C_3 and the best plane containing C_{3a}–C_4–C_5–C_6–C_7–C_{7a} of 12.4° for **5** and 13.6° for **5'** are consistent with a moderate distortion compared to a range of reported indenyl complexes [37,38,43,44,46,47].

2.3. *Spectroscopic characterization of the monosubstituted complexes (η^5-indenyl)(I)(R)(L)Co (3,4,6–12)*

The structures of the monosubstituted complexes (η^5-indenyl)(I)(R)(L)Co (**3,4,6–12**) prepared in this study were established from ^{31}P, ^{1}H, and ^{13}C NMR data (*cf.* Tables 4, 5). ^{31}P NMR spectra (Table 4) show a characteristic singlet corresponding to coordinated phosphine. The ^{31}P complexation shifts ($\Delta(\delta_{complex} - \delta_{free})$) increase with increasing (positive) chemical shift of the free ligand [48]. Comparison of the isostructural pairs **3/4**, **6/7**, **8/9** and **10/11** shows that the perfluoroalkyl ligand has no effect on the ^{31}P chemical shift.

The presence of a chiral Co centre in (η^5-indenyl)(I)(R)(L)Co requires that the indenyl ring atoms (1,3; 4,7; 5,6, *cf.* Scheme 1) be diastereotopic and in general well resolved resonances were observed in both the 7.05 T ^{1}H and ^{13}C NMR spectra. ^{1}H NMR assignments (*cf.* Table 4) are based on nuclear Overhauser effect difference (nOed) spectra shown in Fig. 2 for the representative case of complex **3** and are supported by 2-D ^{1}H/^{13}C ^1J heterocorrelation spectra. Irradiation of the proton resonance at $\delta = 5.11$ ppm (Fig. 2(g)) results in 1.6% enhancement of the peak at $\delta = 5.83$ ppm and 1.2% enhancement of the peak at $\delta = 7.37$ ppm, but no enhancement to the peak at 6.67 ppm. Irradiation of the proton resonance at $\delta = 5.83$ ppm (Fig. 2(f)) shows a 1.8% enhancement at $\delta = 5.11$ ppm and a 2.8% enhancement at $\delta = 6.67$ ppm, respectively. Irradiation of the proton at $\delta = 6.67$ ppm (Fig. 2(e)) results in 1.6% enhancement of the proton at $\delta = 5.83$ ppm and 2.0% enhancement of the proton at $\delta = 7.67$ ppm, respectively. Accordingly the three indenyl signals in the region of 5.0–7.0 ppm are assigned to H_1 (5.11 ppm), H_2 (5.83 ppm), H_3 (6.67 ppm), respectively. The higher field doublet ($\delta = 7.37$ ppm) is assigned to H_7 while the lower field doublet ($\delta = 7.67$ ppm) corresponds to H_4 (*cf.* Scheme 1 for numbering system). The assignment of H_5 (7.32 ppm) and H_6 (7.52 ppm) follows from Fig. 2(a,b) and is confirmed by 2-D ^{1}H/^{13}C heterocorrelation spectra. ^{1}H NMR spectra for the remaining complexes were assigned by comparison with complex **3**. Assignments for well resolved phenyl proton resonances were confirmed by nOed evidence using the method described by Coville [49–51].

The ^{13}C spectra of these complexes (*cf.* Table 5) were unambiguously assigned on the basis of 2-D ^{1}H/^{13}C ^1J heterocorrelation spectra. In the case of complex **3**, the correlations ^{13}C (96.47 ppm) with H_2 ($\delta = 5.83$ ppm), ^{13}C (81.08 ppm) with H_3 ($\delta = 6.67$ ppm) and ^{13}C (65.36 ppm) with H_1 ($\delta = 5.11$ ppm) assign the indenyl carbon atoms as C_1 ($\delta = 65.36$ ppm), C_2 ($\delta = 96.47$ ppm) and C_3 ($\delta = 81.08$ ppm), respectively. Correlations of H_4–H_7 with C_4–C_7 were also clearly observed so that the assignments of the remaining indenyl carbons presented in Table 5 are unambiguous. Assignments for the remaining complexes in the series were made analogously. Characteristic chemical shift patterns were observed for the phenyl ring carbons, hence assignments are based on a combination of 2-D ^{1}H/^{13}C heterocorrelations and comparison of their $C^{13}\{^1H\}$ spectra.

The ^{19}F chemical shifts and coupling constants for the complexes investigated in this study are reported in Table 6. As found previously [44], all complexes showed

TABLE 3. Selected bond distances (Å) and bond angles (°) for [(η^5-C_9H_7)(C_3F_7)(PMe_3)$_2$Co]$^+$ I^- (**5** and **5'**)

5		**5'**	
Distances			
Co(1)–P(1)	2.273(3)	Co(1')–P(1')	2.274(3)
Co(1)–P(2)	2.214(3)	Co(1')–P(2')	2.245(3)
Co(1)–C(1)	2.092(8)	Co(1')–C(1')	2.091(8)
Co(1)–C(2)	2.082(8)	Co(1')–C(2')	2.065(8)
Co(1)–C(3)	2.099(9)	Co(1')–C(3')	2.097(8)
Co(1)–C(3A)	2.235(8)	Co(1')–C(3A')	2.259(8)
Co(1)–C(7A)	2.261(8)	Co(1')–C(7A')	2.288(8)
Co(1)–C(8)	1.961(9)	Co(1')–C(8')	1.971(9)
C(1)–C(2)	1.41(1)	C(1')–C(2')	1.41(1)
C(1)–C(7A)	1.44(1)	C(1')–C(7A')	1.42(1)
C(2)–C(3)	1.39(1)	C(2')–C(3')	1.40(1)
C(3)–C(3A)	1.44(1)	C(3')–C(3A')	1.43(1)
C(3A)–C(7A)	1.43(1)	C(3A')–C(7A')	1.44(1)
Angles			
P(1)–Co(1)–P(2)	97.3(1)	P(1')–Co(1')–P(2')	97.1(1)
P(1)–Co(1)–C(1)	156.3(3)	P(1')–Co(1')–C(1')	155.0(3)
P(1)–Co(1)–C(2)	126.9(3)	P(1')–Co(1')–C(2')	120.6(3)
P(1)–Co(1)–C(3)	92.8(3)	P(1')–Co(1')–C(3')	89.2(3)
P(1)–Co(1)–C(3A)	92.5(2)	P(1')–Co(1')–C(3A')	95.5(2)
P(1)–Co(1)–C(7A)	123.7(2)	P(1')–Co(1')–C(7A')	129.1(3)
P(1)–Co(1)–C(8)	90.8(3)	P(1')–Co(1')–C(8')	91.8(3)
P(2)–Co(1)–C(1)	99.6(3)	P(2')–Co(1')–C(1')	102.9(3)
P(2)–Co(1)–C(2)	84.4(3)	P(2')–Co(1')–C(2')	142.1(3)
P(2)–Co(1)–C(3)	108.1(3)	P(2')–Co(1')–C(3')	149.9(3)
P(2)–Co(1)–C(3A)	146.1(2)	P(2')–Co(1')–C(3A')	111.8(2)
P(2)–Co(1)–C(7A)	137.8(2)	P(2')–Co(1')–C(7A')	90.0(2)
P(2)–Co(1)–C(8)	96.2(3)	P(2')–Co(1')–C(8')	96.3(3)
C(1)–Co(1)–C(8)	103.7(4)	C(1')–Co(1')–C(8')	100.7(4)
C(2)–Co(1)–C(8)	142.0(4)	C(2')–Co(1')–C(8')	87.5(4)
C(3)–Co(1)–C(8)	154.7(3)	C(3')–Co(1')–C(8')	113.0(4)
C(3A)–Co(1)–C(8)	116.1(3)	C(8A')–Co(1')–C(8')	149.8(3)
C(7A)–Co(1)–C(8)	93.2(3)	C(7A')–Co(1')–C(8')	137.6(3)

well separated C_α–C_γ and C_α–C_ζ resonances for the perfluoropropyl and perfluorohexyl groups. The presence of the chiral Co centre and typically small vicinal couplings (^3J(FF) = 5–10 Hz) allows approximation of the diastereotopic $(CF_2)_n$ groups as a series of isolated AB spin systems. Table 7 collects the coupling constants $^2J(F_aF_b)$ and diastereotopic chemical shift differences $\Delta\delta(F_b–F_a)$ for F_a–C_i–F_b for the (η^5-indenyl)(I)(R)(L)Co complexes prepared in this study and reported previously [43,44]. Geminal coupling $^2J(F_aF_b)$ shows a marked increase on passing from C_α to C_β but remains relatively constant further along the perfluoroalkyl chain (*cf.* Fig. 3) consistent with a weakening of the C_α–F bond [52]. The diastereotopic chemical shift difference $\Delta\delta(F_b–F_a)$ for those complexes with strongly anisotropic substituents (L = CO or PPh_nR_{3-n}, n = 1, 2, 3, entries A–K) shows a maximum at C_β (Fig. 4(a)) except for the case with L = PPh_2(OMe) (**11**, entry H), however the trimethylphosphite or trimethylphosphine derivatives show a monatomic decrease for $\Delta\delta(F_b - F_a)$ (Fig. 4b) with increasing distance from the chiral cobalt centre.

2.4. Solution conformation of the monosubstituted complexes (η^5-indenyl)(I)(R)(L)Co (3,4,6–12)

The solution conformation of the monosubstituted derivatives **3**, **4**, **6–12** was studied using ^{1}H nuclear Overhauser effect difference spectroscopy (nOed). The nOed spectra of complexes **3** and **7** (*cf.* Figs. 2 and 5) are representative. The data of Fig. 2 unambiguously show that the PMe_3 ligand bisects the indenyl H_1 and H_7 protons. Irradiation of the Me groups results in a strong enhancement to H_1 (1.7%) and H_7 (3.0%), and a very weak enhancement to H_2 (0.5%), H_3 (0.4%) and H_4 (0.3%) (*cf.* Fig. 2(h)). The nOed spectra of complex **7** (*cf.* Fig. 5) are also in accord with the conformational arguments presented above. Irradiation of the *ortho*-proton resonances of the $PPhMe_2$ ligand results in strong enhancements for H_7 (2.6%), H_1 (3.7%), and the diastereotopic PMe_2 groups (2.0% and 2.3%) (*cf.* Fig. 5(a)). Irradiation of H_7 results in enhancement of the *ortho*-protons (1.8%), H_1 (4.9%), and the diastereotopic Me groups (0.9% and 1.2%), respectively (*cf.* Fig. 5(f)). The diastereotopic PMe_2 groups could not be saturated with complete selectivity, however,

TABLE 4. ^{1}H and ^{31}P NMR for η^5-indenyl Co^{III} complexes [a–c]

Compound	H_1	H_2	H_3	H_4	H_5	H_6	H_7	C_6H_5	Me	^{31}P	$\Delta(\delta_{MP} - \delta_P)$
3	5.11	5.83	6.67	7.67 (d, 8.4)	7.32 (t, 8.5)	7.52 (t, 7.8)	7.37 (d, 8.9)		1.38 (d, 12.2)	8.35	68.89
4	5.12	5.83	6.67	7.67 (d, 8.4)	7.32 (t, 8.3)	7.52 (t, 7.6)	7.37 (d, 9.0)		1.39 (d, 10.8)	8.39	68.93
5 [d]	6.34 (d, 2.7) [e]	6.09	6.34 (d, 2.7) [e]	7.90 (m)	7.77 (m)	7.77 (m)	7.90 (m)		1.71 (t, 5.6)	12.50	73.04
6	4.57	5.61	6.55	7.50 [f]	7.22 (t, 8.3)	7.06 (t, 8.2)	6.35 (d, 8.4)	7.50 (m) [g] 7.75 (m) [h]	1.81 (d, 9.7) 1.73 (d, 9.9)	12.33	57.27
7	4.58	5.60	6.56	7.50 [f]	7.21 (t, 7.6)	7.06 (t, 7.8)	6.33 (d, 8.3)	7.50 (m) [g] 7.76 (m) [h]	1.83 (d, 10.7) 1.75 (d, 10.6)	12.21	57.15
8	4.94	5.70	6.68	7.40 [f]	7.26 (t, 7.5)	6.96 (t, 7.6)	6.30 (d, 8.4)	[i]	2.02 (d, 10.1)	23.71	50.07
9	4.96	5.69	6.67	7.40 [f]	7.26 (t, 7.6)	6.95 (t, 7.6)	6.29 (d, 8.5)	[i]	2.03 (d, 10.2)	23.84	50.20
10	4.74	5.67	6.47	[f]	[f]	[f]	6.85 (m)	7.06–7.52 (m)	3.29 (d, 10.8)	141.98	24.60
11	4.85	5.75	6.55	[f]	[f]	[f]	6.94 (m)	7.14–7.60 (m)	3.37 (d, 9.9)	141.74	24.36
12	4.40	6.02	6.75	7.82 (d, 8.2)	[f]	[f]	6.22 (d, 8.3)	7.10–7.53 (m)		34.73	39.66

[a] ^{1}H (300.1 MHz) NMR chemical shifts in ppm relative to TMS; ^{31}P (121.5 MHz) NMR chemical shifts in ppm relative to external 85% H_3PO_4; ^{31}P NMR of free ligands in $CDCl_3$: PMe_3, −60.54; $PPhMe_2$, −44.94; PPh_2Me, −26.36; PPh_3, −4.93; PPh_2(OMe), 117.38. Solvent = $CDCl_3$; m, multiplet; d, doublet; t, triplet; J values in Hz given in brackets. [b] Coupling constants of indenyl protons (H_4–H_7) are ^3J(HH); Coupling constants for Me are J(PH). [c] All indenyl proton peaks show further small, unresolved coupling (0.3–1.5 Hz). [d] solvent = acetone-d_6. [e] J(PH). [f] Overlapped with phenyl resonances. [g] H_{meta}, H_{para}. [h] H_{ortho}. [i] Two phenyl signals appear as two multiplets at 7.36–7.51 and 7.54–7.64 ppm, respectively.

Fig. 5(i, j) shows that irradiation of the higher and lower field diastereotopic resonances (*cf.* Fig. 5(i, j)) led to strong enhancements to H_1 (2.7%, 3.4%) and H_7 (3.4%, 2.4%) but weaker enhancement to H_2 (1.5%, 1,3%) and H_3 (0.7%, 0.4%). Successive irradiation of H_1, H_2, H_3 revealed the proximal protons (Fig. 5(h, g, f)).

Two bond phosphorus/carbon coupling constant data support the same conformational preference. The C_3 resonances which are *trans* to P (*cf.* Table 5) for all complexes with the formula (η^5-indenyl)(I)(R)(L)Co (**3**, **4** and **6–12**) are doublets with ^2J(PC) equal to 8.5 ± 1.5 Hz. No coupling was observed for C_1 which is *cis* to the phosphorus atom. In some cases, coupling of C_2 to phosphorus was also detected.

2.5. *Indenyl distortions of the monosubstituted complexes (η^5-indenyl)(I)(R)(L)Co (3, 4, 6–12)*

Literature evidence suggests that NMR chemical shift parameters are reliable distortion indicators for transition metal organometallic π-indenyl complexes [2,6,36,39,43,44,49,53,54]. The parameter $\Delta\delta^{13}C_{3a,7a}$ ($\Delta\delta^{13}C_{3a,7a} = \delta^{13}C_{3a,7a}$(indenyl) $- \delta^{13}C_{3a,7a}$(Na^+indenyl$^-$)) is diagnostic of indene hapticity [2,6,46,47,55] with values in the range −10 to −40 ppm and +5 to +30 indicating η^5 and η^3 bonding, respectively [6]. The calculated $\Delta\delta^{13}C_{3a,7a}$ parameters, determined as the value for the diastereotopic ring junction carbons of all the chiral complexes **3**, **4** and **6–12** along with literature values of previously reported complexes [43,44] (*cf.* Table 8), are in the range of −23 to −15 ppm consistent with their description as slightly distorted η^5 complexes [6,46].

Both electronic [38,56] and steric [49–51,54] factors of the ancillary ligands appear to influence the extent of η^5-indenyl ring distortion as well as the preferred conformation of the ligands relative to indenyl ring in solution. Tables 4 and 5 show that ^{1}H and ^{13}C chemical shifts of η^5-indenyl are relatively insensitive to the perfluoroalkyl ligand for the complexes prepared in this study since the electronic and steric requirements of C_3F_7 and C_6F_{13} are similar. The observed diastereotopic chemical shifts for the η^5-indenyl H_1/H_3 and C_1/C_3 resonances in complexes **3**, **4**, **6–12**, however, are a function of the stereoelectronic parameters (θ (°) and χ (cm^{-1})) [57,58] of the phosphorus ligand. Comparative data tabulating $\Delta\delta(H_3-H_1)$ and $\Delta\delta(C_3-C_1)$ for the (η^5-indenyl)(I)(R)(L)Co (L = P-donor)

TABLE 5. ^{13}C NMR for η^5-indenyl Co^{III} complexes [a]

Compound	C_1	C_2	C_3	C_{3a}/C_{7a}	C_4	C_5	C_6	C_7	C_6H_5	CH_3
3	65.36	96.47 (d, 6.2)	81.08 (d, 7.6)	111.32, 110.89	130.04	131.70	129.81	123.43		16.99 (d, 32.4)
4	65.46	96.47 (d, 8.3)	81.10 (d, 7.7)	111.35, 110.81	130.06	131.70	129.82	123.43	–	17.01 (d, 32.2)
5 [b]	76.80	99.64	76.80	112.40	127.19	133.50	133.50	127.19		18.61 (t, 16.3)
6	70.50	93.65 (d, 6.4)	77.65 (d, 9.2)	113.30, 108.20	127.65	131.00	130.19	124.08	136.10 [c], 130.58 [d], 130.48 [d] 130.19 [e], 128.53 [f], 128.41 [f]	17.95 (d, 34.8) 16.97 (d, 27.9)
7	70.69	93.73 (d, 7.5)	77.54 (d, 9.6)	113.63, 108.32	127.69	131.10	130.21	124.18	136.10 [c], 130.65 [d], 130.55 [d] 130.21 [e], 128.60 [f], 128.49 [f]	18.16 (d, 35.2) 17.03 (d, 29.9)
8	70.85	93.21	79.09 (d, 8.4)	113.23, 110.04	130.24	131.20	130.98	124.21	133.37 [c], 133.30 [c], 132.98 [d] 132.85 [d], 132.80 [d], 132.67 [d] 130.43 [e], 128.29 [f], 128.14 [f]	18.91 (d, 33.1)
9	70.95	93.16	78.98 (d, 6.9)	113.26, 109.90	130.24	131.24	130.96	124.27	134.03 [c], 133.47 [c], 132.93 [d] 132.80 [d], 132.68 [d], 130.41 [e] 128.16 [f], 128.04 [f]	19.00 (d, 33.1)
10	71.36	95.07	80.37 (d, 9.4)	113.97, 111.84	130.92	131.37	131.11	125.27	134.70 [c], 134.16 [c], 133.20 [d] 133.06 [d], 132.80 [d], 132.66 [d] 131.11 [e], 127.80 [f], 127.64 [f] 127.50 [f]	56.61 (d, 10.5)
11	71.36	95.12	80.25 (d, 10.2)	113.93, 111.79	130.86	131.32	131.03	125.27	134.65 [c], 134.20 [c], 133.20 [d] 133.07 [d], 132.70 [d], 132.56 [d] 131.03 [e], 127.73 [f], 127.57 [f] 127.43 [f]	56.54 (d, 5.2)
12	72.84	95.76 (d, 9.4)	78.37 (d, 9.5)	114.96, 112.24	128.05	132.03	131.27	124.44	134.90 [c], 133.05, 132.90 131.50, 130.31, 129.15 127.65, 127.53	

[a] ^{13}C (75.47 MHz) NMR chemical shifts in ppm relative to solvent $CDCl_3$ = 77.0; d, doublet; *J* values in Hz given in brackets, *J*(PC); perfluoroalkyl carbons distributed in the chemical shift range of 105–140 ppm with very weak intensity. [b] Solvent = acetone-d_6 (29.8, 206.0 ppm). [c] C_{ipso} (d, ^1J(PC) = 45.52 Hz). [d] C_{ortho}. [e] C_{para}. [f] C_{meta}.

TABLE 6. ^{19}F NMR for η^5-indenyl Co^{III} complexes [a]

Compound	$C_\alpha F_2$ F_a, F_b	$C_\beta F_2$ F_a, F_b	$C_\gamma F_2$ F_a, F_b	$C_\delta F_2$ F_a, F_b	$C_\epsilon F_2$ F_a, F_b	CF_3
3	−55.76, −65.68 (d, 233.8)	−112.95, −115.24 (d, 280.9)				s − 79.31 (t, 12.4)
4	−54.42, −65.57 (d, 234.2)	−107.74, −111.87 (d, 288.0)	−120.63, −122.01 (d, 299.32)	−122.48, −123.60 (d, 306.5)	−126.09, −127.04 (d, 293.3)	−81.32 (t, 9.5)
5 [b]	−71.09	−112.84				−78.16 (t, 12.32)
6	−58.94, −58.94	−108.29, −113.82 (d, 277.9)				−79.59 (t, 10.5)
7	−57.77, −58.58 (d, 227.9)	−103.56, −110.23 (d, 284.5)	−120.90, −122.06 (d, 292.9)	−122.89, −122.89	−126.53, −126.53	−81.27 (t, 10.8)
8	−57.35, −58.16 (d, 227.7)	−109.18, −112.86 (d, 276.87)				−79.76 (t, 10.8)
9	−56.67, −57.21 (d, 229.2)	−104.80, −108.97 (d, 283.5)	−121.62, −121.62	−122.95, −122.95	−126.60, −126.60	−81.30 (t, 9.9)
10	−55.71, −57.33 (d, 228.4)	−109.81, −111.65 (d, 278.0)				−79.88
11	−54.22, −56.99 (d, 222.5)	−106.71, −106.71	−121.13, −122.40 (d, 295.0)	−122.57, −123.34 (d, 290.1)	−126.22, −127.01 (d, 293.6)	−81.30
12	−54.05, −54.73 (d, 224.9)	−108.47, −111.62 (d, 274.5)				−80.02

[a] 282.4 MHz, chemical shifts in ppm relative to $CFCl_3$; solvent = $CDCl_3$; $^2J(F_aF_b)$, and $^3J(FF)$ in the case of CF_3, in Hz given in brackets; all CF_2 peaks show further unresolved coupling of *ca.* 5–10 Hz (^3J and ^4J). [b] Solvent = acetone − d_6.

complexes reported in this work and several examples taken from the literature [43,44] are given in Table 8 and Fig. 6.

Faller and Crabtree [38,56] have convincingly argued that preferential weakening of the Co–C_{3a} and Co–C_{7a} bonds will facilitate more significant stabilization *via* aromatization hence strong *trans*-influence ligands will prefer a site *trans* to the indenyl 6-ring regardless of steric consequences. This rationale predicts that strong *trans*-influence perfluoroalkyl ligands in complexes **3**, **4**, **6–12** will select a conformation placing L between H_1 and H_7, *trans* to H_3 of the indenyl ring as shown in Scheme 1. As a consequence, the chemical shifts of H_2/C_2 are relatively insensitive to P-donor stereoelec-

TABLE 7. Correlation of ^{19}F NMR parameters with ligand properties for (η^5-indenyl)(R)(I)(L)Co complexes [a]

L	R	$C_\alpha F_aF_b$		$C_\beta F_aF_b$		$C_\gamma F_aF_b$		$C_\delta F_aF_b$		$C_\epsilon F_aF_b$		[b]	Ref.
		$\Delta\delta(F_b-F_a)$	$^2J(F_aF_b)$	$\Delta\delta(F_b-F_a)$	$^2J(F_aF_b)$	$\Delta\delta(F_b-F_a)$	$^2J(F_aF_b)$	$\Delta\delta(F_b-F_a)$	$^2J(F_aF_b)$	$\Delta\delta(F_b-F_a)$	$^2J(F_aF_b)$		
CO	C_3F_7	3.56	208.1	3.76	278.0							A	[c]
CO	C_6F_{13}	2.16	210.6	6.07	286.6	1.75	298.8	1.07	300.9	1.11	294.5	B	[c]
$PPh(OMe)_2$	C_3F_7	0.56	229.9	2.95	279.1							C	[c]
PNH [d]	C_3F_7	0.40	247.6	4.33	277.3							D	[c]
PPh_2Me	C_3F_7	0.81	227.7	3.68	276.9							E	[e]
PPh_2Me	C_6F_{13}	0.54	229.2	4.17	283.5	0	–	0	–	0	–	F	[e]
$PPh_2(OMe)$	C_3F_7	1.62	228.4	1.84	278.0							G	[e]
$PPh_2(OMe)$	C_6F_{13}	2.77	222.5	0	–	1.27	295.0	0.77	290.1	0.79	293.6	H	[e]
$PPhMe_2$	C_3F_7	0	–	4.91	277.9							I	[e]
$PPhMe_2$	C_6F_{13}	0.81	227.8	6.67	284.5	1.16	292.9	0	–	0	–	J	[e]
PPh_3	C_3F_7	0.70	224.9	3.15	274.5							K	[e]
$P(OMe)_3$	C_3F_7	7.08	228.3	1.65	281.2							M	[c]
$P(OMe)_3$	C_6F_{13}	8.28	230.6	3.55	284.0	1.22	295.3	1.01	307.8	1.00	294.6	N	[c]
PMe_3	C_3F_7	9.92	233.8	2.29	280.9							O	[e]
PMe_3	C_6F_{13}	11.15	234.2	4.13	288.0	1.38	299.3	1.12	306.5	0.95	293.3	P	[e]

[a] $\Delta\delta(F_b-F_a) = \delta_{F_b} - \delta_{F_b}$ in ppm; $^2J(F_aF_b)$ in Hz. [b] Legend used in Figs. 3 and 4. [c] Data from reference [44]. [d] PNH = (*S*)-$PPh_2NHC^*H(Me)Ph$. [e] This work.

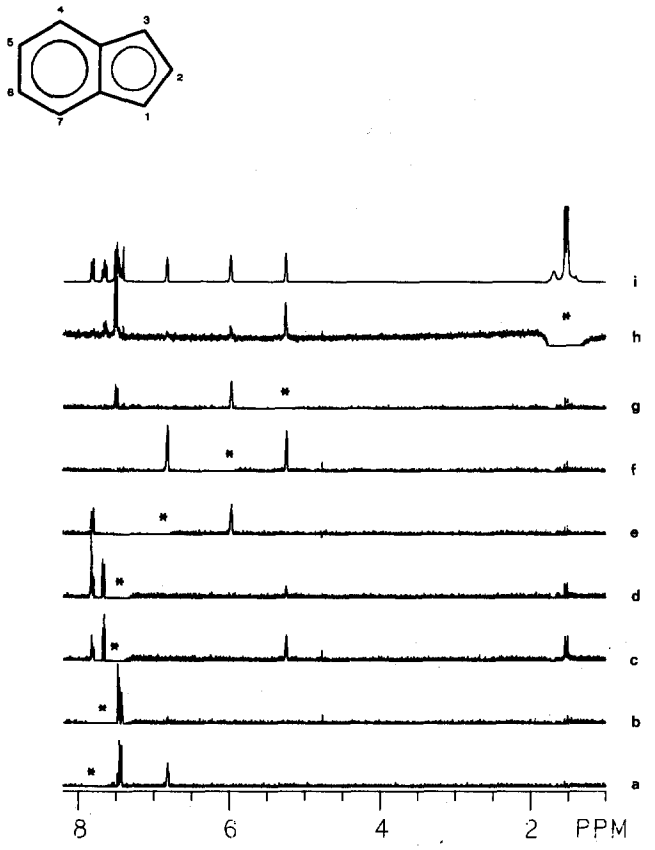

Fig. 2. ^{1}H nOed spectra for (η^5-C_9H_7)(C_3F_7)(I)(PMe_3)Co (3). (i) Reference spectrum; (a–h) difference spectra (64×) for irradiation at the indicated (*) frequency; (a) H_4; (b) H_6 (c,d) H_7 and H_5; (e) H_3; (f) H_2; (g) H_1; (h) Me.

tronic parameters while the chemical shifts of H_1/C_1 and H_3/C_3, which are *cis* and *trans* to L, respectively, correlate with P-donor stereoelectronic parameters as

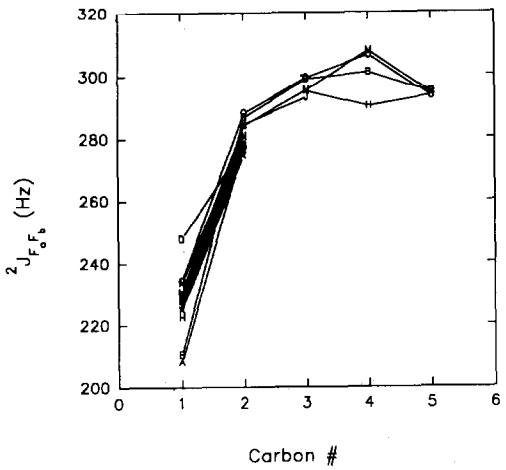

Fig. 3. Dependence of the ^{19}F coupling constants on position for (η^5-indenyl)(R)(I)(L)Co complexes (*cf.* Table 7 for legend).

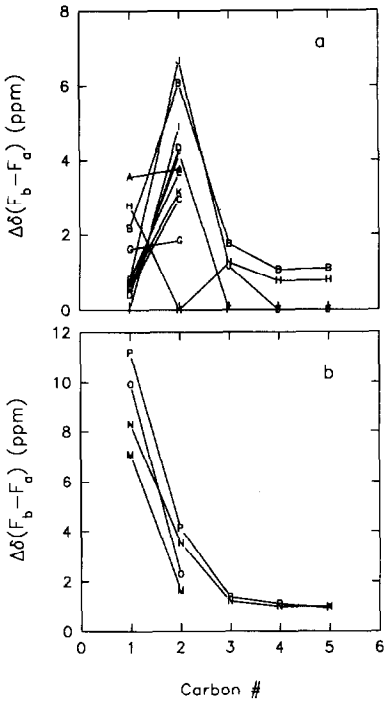

Fig. 4. Dependence of diastereotopic ^{19}F chemical shift difference $\Delta\delta(F_b-F_a)$ on position for (η^5-indenyl)(R)(I)(L)Co Complexes (*cf.* Table 7 for legend).

observed in this study (*cf.* Fig. 6) and demonstrate that a preferred rotamer is adopted by these chiral complexes in solution.

The preferred conformation of the high *trans*-influence perfluoroalkyl ligands in this series of η^5-indenyl complexes results in weakening of the cobalt-ring junction carbon bond. The latter causes distortion of η^5-indenyl ring and the former renders the diastereotopic chemical shifts for indenyl ^{1}H and ^{13}C sensitive to the ligands. Accordingly, the diastereotopic chemical shift differences $\Delta\delta(H_3-H_1)$ and $\Delta\delta(C_3-C_1)$ may provide an internal measurement of indenyl distortion in chiral complexes. Figure 7 correlates the parameters $\Delta\delta(H_3-H_1)$ and $\Delta\delta(C_3-C_1)$ with $\Delta\delta^{13}C_{3a,7a}$ and suggests that diastereotopic chemical shift differences are an alternative indicator of indenyl ring distortion.

3. Experimental section

3.1. Reagents and methods

All manipulations were performed under a dry, oxygen-free nitrogen atmosphere using standard Schlenk techniques. Nitrogen gas was purified by passing through a series of columns containing DEOX (Alpha) catalyst heated to 120°C, granular P_4O_{10}, and finally activated 3 Å molecular sieves. Benzene and hexane

solvents were distilled under nitrogen from blue solutions of sodium benzophenone ketyl. Methylene chloride was distilled under nitrogen from P_4O_{10} and acetone from 4 Å molecular sieves (4–8 mesh). PMe_3, $PPhMe_2$, PPh_2Me, $PPh_2(OMe)$ and PPh_3 were purchased from Strem and used as received. Thin layer chromatographic (TLC) analyses were performed on pre-coated analytical TLC plates (silica gel F-254, Merck). Chromatographic separations were carried out using a Chromatotron (Harrison Associates) with 4 mm thick silica $gel_{60}PF_{254}$ (Merck) adsorbent. Elemental analyses were performed by Canadian Microanalytical Service Ltd. (Delta, B.C.). Melting points were determined in nitrogen sealed capillaries and are uncorrected. NMR spectra were recorded on a GE 300-NB Fourier transform spectrometer operating at a proton frequency of 300.12 MHz. Complexes **1** and **2** were prepared as described previously [43,44].

Proton nOed spectra were determined under steady state conditions on the GE 300-NB instrument. Data were collected at 25.0°C using interleaved experiments of 16 or 32 transients cycled 12–16 times through the list of decoupling frequencies. In each experiment, the decoupler was gated in continuous wave (CW) mode for 2s with sufficient attenuation to give an approximate 70–90% reduction in intensity of the irradiated peak. A 30 s delay preceded each frequency change. A set of four dummy scans was employed to equilibrate the spins prior to data acquisition. No relaxation delay was applied between successive scans of a given decoupling frequency. Difference spectra were obtained on 16K or zero-filled 32K data tables which had been

TABLE 8. Distortion, electronic and stereochemical parameters for the (η^5-indenyl)(I)(R)(L)Co complexes [a]

L	R	$\Delta\delta(H_3-H_1)$ [b]	$\Delta\delta(C_3-C_1)$ [c]	$\Delta\delta(C_{3a,7a})$ [d] (ave.)	θ(°) [e]	χ (cm^{-1}) [e]
PMe_3	C_3F_7	1.56	15.72	−19.38, −19.81 (−19.60)	118	8.55
PMe_3	C_6F_{13}	1.55	15.64	−19.35, −19.89 (−19.62)	118	8.55
$PPhMe_2$	C_3F_7	1.98	7.15	−17.40, −22.50 (−19.95)	122	10.60
$PPhMe_2$	C_6F_{13}	1.98	6.85	−17.07, −22.38 (−19.73)	122	10.60
PPh_2Me	C_3F_7	1.74	8.24	−17.47, −20.66 (−19.07)	136	12.10
PPh_2Me	C_6F_{13}	1.71	8.03	−17.44, −20.80 (−19.12)	136	12.10
$PPh_2(OMe)$	C_3F_7	1.73	9.01	−16.73, −18.86 (−17.80)	132	16.30
$PPh_2(OMe)$	C_6F_{13}	1.70	8.89	−16.77, −18.91 (−17.84)	132	16.30
PPh_3	C_3F_7	2.35	5.53	−15.74, −18.46 (−17.10)	145	13.25
CO	C_3F_7	1.04	16.09	−19.05, −21.24 (−20.14)	–	–
CO	C_6F_{13}	1.05	16.01	−19.07, −21.25 (−20.16)	–	–
$PPh(OMe)_2$	C_3F_7	1.59	9.10	−17.00, −20.78 (−18.89)	120	19.45
$PPh(OMe)_2$	C_6F_{13}	1.55	8.84	−17.05, −20.77 (−18.91)	120	19.45
$P(OMe)_3$	C_3F_7	1.11	13.11	−18.36, −20.51 (−19.44)	107	24.10
$P(OMe)_3$	C_6F_{13}	1.09	12.85	−18.42, −20.48 (−19.45)	107	24.10
PNH [f]	C_3F_7	2.13	6.01	−18.17, −18.99 (−18.58)	140	10.50
PNH [f]	C_6F_{13}	2.11	5.64	−17.92, −19.43 (−18.68)	140	10.50

[a] Data in the lower part of this table, see references [43,44]. [b] $\Delta\delta(H_3-H_1)=\delta(H_3)-\delta(H_1)$ (ppm). [c] $\Delta\delta(C_3-C_1)=\delta(C_3)-\delta(C_1)$ (ppm). [d] $\Delta\delta(C_{3a,7a})=\delta[C_{3a,7a}(\text{indenyl})-\delta[C_{3a,7a}Na^+\text{indenyl}^-)]$, $\delta[C_{3a,7a}(Na^+\text{indenyl}^-)]=130.70$ ppm [6,46]. [e] Parameters obtained from [57,58]. [f] PNH = *S*-$PPh_2NHCH(Me)Ph$.

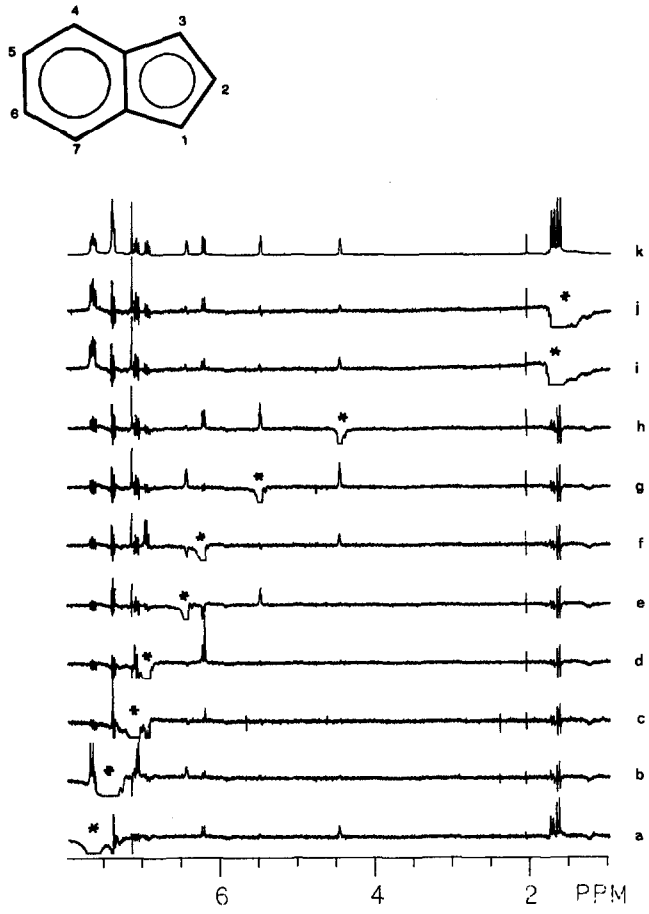

Fig. 5. ^{1}H nOed spectra for $(\eta^5$-indenyl)(I)(C_6F_{13})(PPhMe$_2$)Co (7). (k) Reference spectrum; (a–j) difference spectra (32×) for irradiation at the indicated (*) frequency; (a) H_{ortho}; (b) H_4, H_{meta} and H_{para}; (c) H_5; (d) H_6; (e) H_3; (f) H_7; (g) H_2; (h) H_1; (i, j) Me.

digitally filtered with a 0.1 Hz exponential or Gaussian line broadening function. Quantitative data were obtained by integration.

3.2. *Crystal structure determination of* $[(\eta^5\text{-}C_9H_7)Co(C_3F_7)(PMe_3)_2]I \cdot 0.5\ CH_2Cl_2$ (5)

Crystal data were collected at ambient temperature on a Rigaku AFC6S diffractometer with graphite monochromated Mo Kα radiation, $\lambda = 0.71069$ Å, and a 2 kW sealed tube generator using the ω scan technique to a maximum 2θ value of 45.0°. Cell constants and an orientation matrix for data collection were determined from least squares refinement using the setting angles of the 18 carefully centred reflections in the range $29.25 < 2\theta < 34.76°$ and are given in Table 9. The space group $P2_1/n$ (no. 14) was assigned on the basis of systematic absences ($h0l$, $h + 1 \neq 2n$ and $0k0$, $k \neq 2n$) and on the successful solution and refinement of the structure. Omega scans of several intense reflections, made prior to data collection, had an average

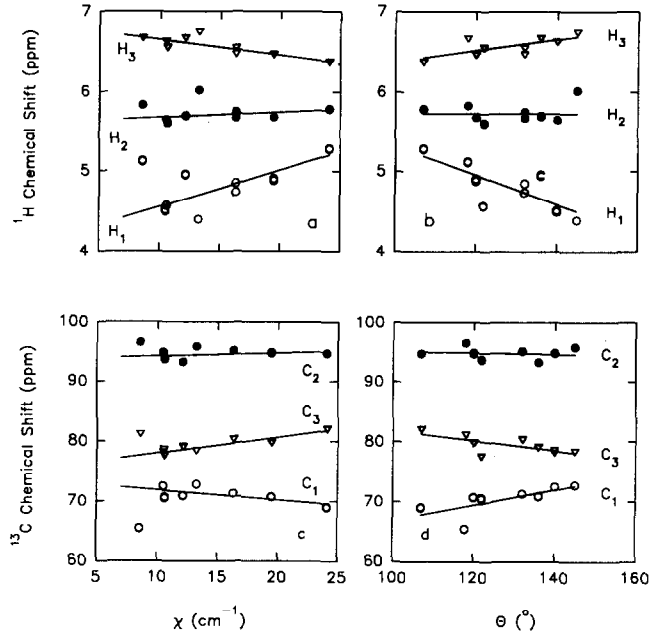

Fig. 6. Correlation of indenyl ^{1}H and ^{13}C chemical shifts with stereoelectronic parameters for $(\eta^5$-indenyl)(R)(I)(L)Co complexes (*cf.* Tables 4, 5, 8 and ref. [44]).

width at half-height of 0.44° with a take-off angle of 6.0°. Scans of $(1.13 + 0.30 \tan\theta)°$ were made at a speed of 8.0°/min (in omega). Weak reflections ($I <$

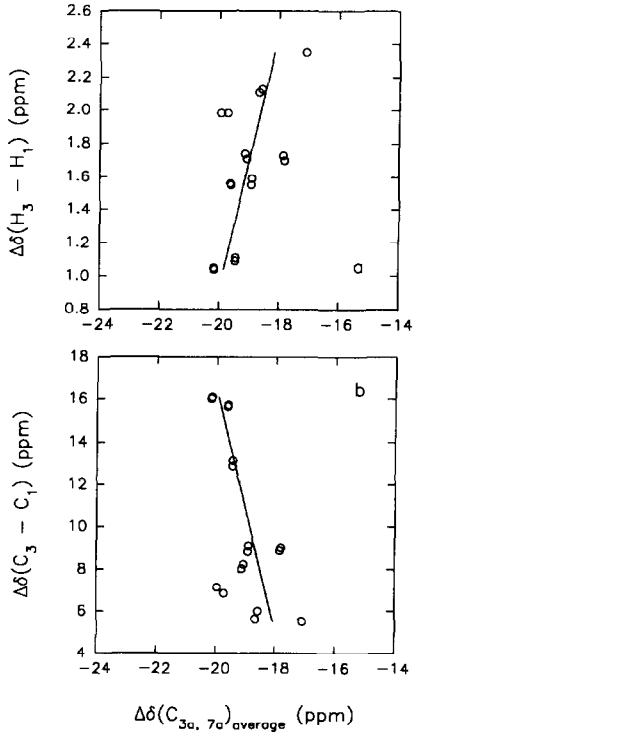

Fig. 7. Correlation between the indenyl distortion parameters for $(\eta^5$-indenyl)(R)(I)(L) complexes (*cf.* Table 8).

TABLE 9. Summary of crystallographic data for **5**

Formula	$C_{37}H_{52}Co_2F_{14}I_2P_4Cl_2$
F.W.(g/mol)	1329.27
Crystal habit	Deep-red prism
Crystal size (mm)	0.35×0.25×0.15
Crystal system	Monoclinic
No. reflections used for unit cell determination (2θ range)	18 (29.3–34.8°)
Omega scan peak width at half-height	0.44
Lattice parameters	
a (Å)	16.760(5)
b(Å)	10.614(7)
c(Å)	28.595(5)
β (°)	96.61(2)
V (Å^3)	5053(3)
Space group	$P2_1/n$ (No. 14)
Z	4
D_{calcd} (g cm^{-3})	1.747
F_{000}	2616
μ(Mo Kα) (cm^{-1})	21.73
Scan width (°)	1.13+0.30 tan θ
$2\theta_{max}$ (°)	45.0
No. reflections measured	
Total	7295
Unique	7015
R_{int}	0.029
Corrections [a]	Lorentz-polarization absorption
trans factors	0.87–1.00
Secondary extinction coefficient	0.27596×10^{-7}
Function minimized	$\Sigma w(\|F_o\|-\|F_c\|)^2$
Least-squares weights	$4F_o^2/\sigma^2(F_o^2)$
p-factor	0.01
Anomalous dispersion	All non-hydrogen atoms
No. observations ($I > 3.00\sigma(I)$)	4097
No. variables	551
Reflection/parameter ratio	7.44
R [b]	0.040
R_w [c]	0.036
Goodness of fit indicator [d]	1.56
Max shift/error in final cycle	0.00
Maximum peak in final diff. Map (e Å^{-3})	1.09
Minimum peak in final diff. Map (e Å^{-3})	−0.66

[a] *cf.* Ref. [60]. [b] $R = \Sigma\|F_o\|-|F_c\|/\Sigma|F_o|$. [c] $R_w = [(\Sigma w(|F_o|-|F_c|)^2/\Sigma wF_o^2)]^{1/2}$. [d] GOF $= (\Sigma(|F_o|-|F_c|)/\sigma)/(n-m))$ where n = no. of reflections, m = no. of variables and σ^2 = variance of $(|F_o|-|F_c|)$.

$10.0\sigma(I)$) were rescanned (max 2) and the counts accumulated to assure good counting statistics. The intensities of three representative reflections were measured after every 150 reflections remained constant throughout the data collection hence no decay corrections were applied. The linear absorption coefficient for Mo Kα is 21.7 cm^{-1}. An empirical absorption correction, based on azimuthal scans of several reflections, was applied resulting in transmission factors ranging from 0.87 to 1.00. The data were corrected for Lorentz and polarization effects. A correction for secondary extinction (coefficient = 0.27596×10^{-7}) was applied. The structure was solved by direct methods [59] using the Molecular Structure Corporation TEXSAN software. Non-hydrogen atoms were refined anisotropically. Idealized hydrogen atoms were included at the calculated positions and were not refined. Further details are given in Table 9.

3.3. Synthesis of $(\eta^5$-$C_9H_7)(R)(I)PMe_3)Co$ ($R = C_3F_7$, **3**; C_6F_{13}, **4**)

These two complexes were synthesized using the procedure described below. A 10-ml benzene solution of PMe_3 (0.03190 g, 0.4193 mmol) was added dropwise with stirring *via* a pressure balanced dropping funnel to a black solution of **2** (0.2503 g, 0.3862 mmol) in 20 ml of benzene at ambient temperature. After stirring for 20 min, the solution was placed in an ice bath for a further 20 min. Removal of volatiles from the deep-red solution under oil pump vacuum left a deep-red powder. The crude product was dissolved in *ca.* 4 ml of acetone and chromatographed on 4 mm silica gel plates. Acetone elution moved a high R_f deep-red zone which was collected. Removal of volatiles with an aspirator and then an oil pump vacuum left a deep-red powder (0.2305 g, 86%). Black rectangular plates were obtained by slow diffusion of hexane onto an acetone solution of **4** at −20°C. A low R_f yellow band was shown (^{1}H NMR) to be a bis-substituted complex with a structure similar to **5**.

3.4. Synthesis of $[(\eta^5$-$C_9H_7)(C_3F_7)(PMe_3)_2Co]^+I^-$ (**5**)

Excess PMe_3 (0.08885 g, 1.168 mmol) was added slowly *via* syringe with stirring to a black solution of **1** (0.2483 g, 0.4985 mmol) in 20 ml of benzene at room temperature. The reaction mixture was stirred for 30 min resulting in a red solution containing some precipitate and then placed on an ice bath for *ca.* 10 min. Removal of volatiles by use of oil pump vacuum left a red powder. The crude product was dissolved in *ca.* 4 ml of acetone and chromatographed on a 4 mm silica gel plate. Acetone elution moved a yellow-red zone which was collected. Removal of solvent by use of a water aspirator and then an oil pump vacuum left a red crystalline powder (0.2915 g, 94%). Deep-red prisms were obtained by slow diffusion of hexane onto the CH_2Cl_2 solution of **5** at −20°C.

3.5. Synthesis of $(\eta^5$-$C_9H_7)(R)(I)(L)Co$ (**6–11**)

Complexes **6–11** were prepared following the procedure described for **6**. In some cases (**6**,**7**,**8**,**9**), the crude product required no further purification. Complexes **10** and **11** were purified by preparative radial TLC (ben-

zene eluent). Reaction yields are reported in Table 1. A slight excess of $PPhMe_2$ (0.05820 g, 0.4213 mmol) was added slowly *via* syringe with stirring to a black solution of **1** (0.1901 g, 0.3817 mmol) in 10 ml of benzene at room temperature. After stirring for 30 min the resulting deep-red solution was cooled in an ice bath for *ca.* 10 min. Removal of volatiles by use of oil pump vacuum gave the crude product as a deep-red powder (0.2130 g, 92%). Black rectangular plates were obtained by slow diffusion of hexane onto a CH_2Cl_2 solution of **6** at −20°C.

3.6. Synthesis of (η^5-C_9H_7)(C_3F_7)(I)(PPh_3)Co (12)

A 10 ml benzene solution of PPh_3 (0.2070 g, 0.7892 mmol) was added dropwise at room temperature with stirring *via* a pressure equalized dropping funnel to a black solution of **1** (0.3215 g, 0.6456 mmol) in 20 ml of benzene. Stirring was continued for 20 min then the brown-red solution containing some uncharacterized green precipitate was filtered through a glass frit and placed in an ice bath for *ca.* 10 min. Removal of volatiles by use of oil pump vacuum left a brown powder which was dissolved in 4 ml of benzene and chromatographed. Benzene/hexane (2 : 1) elution moved a brown zone which was collected. Removal of volatiles by use of aspirator followed by an oil pump vacuum afforded the product as a brown powder (0.1098 g, 23%).

Acknowledgement

We thank the Natural Sciences and Engineering Research Council of Canada (NSERC) for financial support of this work. Z.Z. acknowledges Memorial University for a graduate fellowship.

References

1 E.W. Abel and S. Moorhouse, *J. Chem. Soc., Dalton Trans.*, (1973) 1706.
2 F.H. Kohler, *Chem. Ber., 107* (1974) 570.
3 R. Benn, K. Cibura, P. Hofmann, K. Jonas and A. Rufinska, *Organometallics, 4* (1985) 2214.
4 D.E. Smith and A.J. Welch, *Organometallics, 5* (1986) 760.
5 P. Binger, R. Milczarek, R. Mynott, C. Kruger, Y.-H. Tsay, E. Raabe and M. Regitz, *Chem. Ber., 121* (1988) 637.
6 R.T. Baker and T.H. Tulip, *Organometallics, 5* (1986) 839.
7 N. Piccolrovazzi, P. Pino, G. Consiglio, A. Sironi and M. Moret, *Organometallics, 9* (1990) 3098.
8 B.T. Donovan, R.P. Hughes and H.A. Trujillo, *J. Am. Chem. Soc., 112* (1990) 7076.
9 B.T. Donovan, R.P. Hughes, H.A. Trujillo and A.L. Rheingold, *Organometallics, 11* (1992) 64.
10 N.S. Crossley, J.C. Green, A. Nagy and G. Stringer, *J. Chem. Soc., Dalton Trans.*, (1989) 2139.
11 M.S. Loonat, L. Carlton, J.C.A. Boeyens and N.J. Coville, *J. Chem. Soc., Dalton Trans.*, (1989) 2407.
12 M.A. Huffman and L.S. Liebeskind, *J. Am. Chem. Soc., 112* (1990) 8617.
13 M.A. Huffman, L.S. Liebeskind and W.T. Pennington, *Organometallics, 11* (1992) 255.
14 D. O'Hare, J.C. Green, T. Marder, S. Collins, G. Stringer, A.K. Kakkar, N. Kaltsoyannis, A. Kuhn, R. Lewis, C. Mehnert, P. Scott, M. Kurmoo and S. Pugh, *Organometallics, 11* (1992) 48.
15 M.L.H. Green and A.K. Hughes, *J. Chem. Soc., Dalton Trans.*, (1992) 527.
16 A.J. Hart-Davis and R.J. Mawby, *J. Chem. Soc. A*, (1969) 2403.
17 P. Caddy, M. Green, J.A.K. Howard, J.M. Squire and N.J. White, *J. Chem. Soc., Dalton Trans.*, (1981) 400.
18 P. Caddy, M. Green, E. O'Brien, L.E. Smart and P. Woodward, *J. Chem. Soc., Dalton Trans.*, (1980) 962.
19 L.N. Ji, M.E. Rerek and F. Basolo, *Organometallics, 3* (1984) 740.
20 M.E. Rerek, L.-N. Ji and F. Basolo, *J. Chem. Soc., Chem. Commun.*, (1983) 1208.
21 C.P. Casey and J.M. O'Connor, *Organometallics, 4* (1985) 384.
22 N.N. Turaki, J.M. Huggins and L. Lebioda, *Inorg. Chem.*, 27 (1988) 424.
23 H. Bang, T.J. Lynch and F. Basolo, *Organometallics, 11* (1992) 40.
24 T. Foo and R. a. Bergman, *Organometallics, 11* (1992) 1811.
25 T.C. Forschner, A.R. Cutler and R.K. Kullnig, *Organometallics, 6* (1987) 889.
26 T.C. Forschner, A.R. Cutler and R.K. Kullnig, *J. Organomet. Chem., 356* (1988) C12.
27 T.C. Forschner and A.R. Cutler, *J. Organomet. Chem., 361* (1989) C41.
28 T.C. Forschner and A.R. Cutler, *Organometallics, 4* (1985)1247.
29 S.A. Levitre, A.R. Cutler and T.C. Forschner, *Organometallics, 8* (1989) 1133.
30 T.B. Marder, D.C. Roe and D. Milstein, *Organometallics, 7* (1988)1451.
31 A. Borrini, P. Diversi, G. Ingrosso, A. Lucherini and G. Serra, *J. Mol. Catal., 30* (1985) 181.
32 H. Bonnemann and W. Brijoux, *Aspects Homogeneous Catal., 5* (1984) 75.
33 H. Bonnemann, *Angew. Chem., Int. Ed. Engl., 24* (1985) 248.
34 J.M. O'Connor and C.P. Casey, *Chem. Rev., 87* (1987) 307.
35 G.A. Miller, M.J. Therien and W.C. Trogler, *J. Organomet. Chem., 383* (1990) 271.
36 J.S. Merola, R.T. Kacmarcik and D.V. Engen, *J. Am. Chem. Soc., 108* (1986) 329.
37 R.M. Kowaleski, A.L. Rheingold, W. Trogler C and F. Basolo, *J. Am. Chem. Soc., 108* (1986) 2460.
38 J.W. Faller, R.H. Crabtree and A. Habib, *Organometallics, 4* (1985) 929.
39 A. Habib, R.S. Tanke, E.M. Hot and R.H. Crabtree, *Organometallics, 8* (1989)1225.
40 A.N. Nesmeyanov, N.A. Ustynyuk, L.G. Makarova, V.G. Andrianov, Y.T. Struchkov, S. Andrae, Y.A. Ustynyuk and S.G. Malyugina, *J. Organomet. Chem., 159* (1978) 189.
41 L.P. Szajek, R.J. Lawson and J.R. Shapley, *Organometallics, 10* (1991) 357.
42 H. Ahmed, D.A. Brown, N.J. Fitzpatrick and W.K. Glass, *J. Organomet. Chem., 418* (1991) C14.
43 C.R. Jablonski, Z. Zhou and J.N. Bridson, *J. Organomet. Chem., 429* (1992) 379.
44 C.R. Jablonski and Z. Zhou, *Can. J. Chem., 70* (1992) 2544.
45 A. Salzer and C. Taschler, *J. Organomet. Chem., 294* (1985) 261.
46 S.A. Westcott, A.K. Kakkar, a. Stringer, N.J. Taylor and T.B. Marder, *J. Organomet. Chem., 394* (1990) 777.
47 A.K. Kakker, S.F. Jones, N.J. Talyor, S. Collins and T.B. Marder, *J. Chem. Soc., Chem. Commun.*, (1989) 1454.

48 P.S. Pregosin and R.W. Kunz, *^{31}P and ^{13}C NMR of Transition Metal Phosphine Complexes*, Springer-Verlag, New York, 1979.
49 L. Carlton, P. Johnston and N.J. Coville, *J. Organomet. Chem., 339* (1988) 339.
50 P. Johnston, M.S. Loonat, W.L. Ingham, L. Carton and N.J. Coville, *Organometallics, 6* (1987)$_2$121.
51 M.S. Loonat, L. Carlton, J.C.A. Boeyens and N.J. Coville, *J. Chem. Soc., Dalton Trans.*, (1989) 2407.
52 K.J. Karel, T.H. Tulip and S.D. Ittel, *Organometallics, 9* (1990) 1276.
53 H.P. Fritz and C.G. Kreiter, *J. Organomet. Chem., 4* (1965) 198.
54 M.S. Loonat, L. Carlton and N.J. Coville, *S. Afr. J. Chem., 41* (1988) 72.
55 T.B. Marder, J.C. Calabrese, D.C. Roe and T.H. Tulip, *Organometallics, 6* (1987) 2012.
56 R.H. Crabtree and C.P. Parnell, *Organometallics, 3* (1984)1727.
57 C.A. Tolman, *Chem. Rev., 77* (1977) 313.
58 Hong-Y. Liu, K. Eriks, A. Prock and W.P. Giering, *Organometallics, 9* (1990)1758.
59 C.J. Gilmore, *J. Appl. Crystallogr., 17* (1984) 42.
60 N. Walker and D. Stuart, *Acta Crystallogr. Sect. A, 39* (1983) 158.